RESEARCH ARTICLE

Vegetation-memory effects and their association with vegetation resilience in global drylands

Erik Kusch[1,2] | Richard Davy[3,4] | Alistair W. R. Seddon[1,4]

[1]Institute for Biological Sciences, University of Bergen, Bergen, Norway

[2]Department of Biology, Center for Biodiversity Dynamics in a Changing World (BIOCHANGE), Section for Ecoinformatics & Biodiversity, Arhus University, Aarhus, Denmark

[3]Nansen Environmental and Remote Sensing Center, Bergen, Norway

[4]Bjerknes Center for Climate Change Research, Bergen, Norway

Correspondence
Erik Kusch
Email: erik.kusch@bio.au.dk

Funding information
Bjerknes Fast Track Initiative

Handling Editor: Iain Stott

Abstract

1. Vegetation memory describes the effect of antecedent environmental and ecological conditions on the present ecosystem state and has been proposed as an important proxy for vegetation resilience. In particular, strong vegetation memory has been identified in dryland regions, but the factors underlying the spatial patterns of vegetation memory remain unknown.

2. We aim to map the components and drivers of vegetation memory in dryland regions using state-of-the-art climate reanalysis data and refined approaches to identify vegetation-memory characteristics across dryland regions worldwide.

3. Using a framework which distinguishes between intrinsic and extrinsic ecological memory, we show that (i) intrinsic memory is a much stronger component than extrinsic memory in the majority of dryland regions and (ii) climate reanalysis datasets change the detection of extrinsic vegetation memory in some global dryland regions.

4. *Synthesis.* Our study offers a global picture of the vegetation response to two climate variables using satellite data, information which is potentially relevant for mapping components and properties of vegetation responses worldwide. However, the large differences in the spatial patterns in intrinsic vegetation memory in our study compared to previous analyses show the overall sensitivity of this component to the initial choice of extrinsic predictor variables. As a result, we caution against using the oversimplified link between intrinsic vegetation-memory and vegetation recovery rates at large spatial scales.

KEYWORDS
climate reanalysis, drylands, remote sensing, resilience, vegetation memory

1 | INTRODUCTION

There is a growing concern that future ecosystem-disturbance dynamics will exceed ecological tipping points and cause nonlinear shifts in ecosystem states. Examples of non-linear shifts in ecosystem states include regime shifts from tropical forest to savannas (Senf & Seidl, 2018), from coral-dominated to algae-dominated coral reefs (Nyström & Folke, 2001), and eutrophication and acidification processes in shallow lake ecosystems (Spears et al., 2017). Such regime shifts can have major local and global impacts with consequences for

ecosystem functioning and human well-being (Côté & Darling, 2010; Genkai-Kato, 2007; Scheffer & Carpenter, 2003).

Ecological resilience, the ability of a system to withstand disturbance and maintain its general functioning, is an important property to safeguard against such regime shifts (Holling, 1973). Ecological resilience has been incorporated into the objectives of numerous agencies influential at the global policy level (e.g. Convention on Biological Diversity, 2020), and is a key focus within several of the United Nations Sustainable Development Goals (Sustainable Development Goals, 2020).

Although ecological resilience has been prevalent in the global change literature (Côté & Darling, 2010; Cumming et al., 2015; Neubert & Caswell, 1997), universal baseline metrics on which to assess and compare resilience in different ecosystems are yet to be established (Standish et al., 2014). Consequently, it is impossible to make reliable assessments of resilience and compare ecosystem components through time and space (Pimm et al., 2019). Indeed, although several metrics of resilience have been proposed (i.e. resistance to perturbation, recovery rate from a disturbance and robustness) based on ecological theory (Grafton et al., 2019; Hodgson et al., 2015), a challenge that follows is how to operationalise these metrics with empirical data.

Remote sensing has been proposed to act as a useful tool to map components of resilience to climate variability at large spatial scales by combining data of both ecological response (e.g. vegetation indices) and predictor (e.g. climate) variables. For example, studies of vegetation responses to climate variability using remote-sensing techniques have identified localised patterns of vegetation sensitivity (Seddon et al., 2016), lagged-vegetation response to climatic anomalies (Liu et al., 2018; Vicente-Serrano et al., 2013), vegetation resistance (an inverse proxy of how easily the system is perturbed where an easily perturbed system exhibits low resilience) and engineering resilience (a proxy for how quickly a perturbed system returns to its pre-disturbance state) (De Keersmaecker et al., 2015).

One important feature of studies which use remote-sensing data to map components of ecological resilience worldwide is the quantification of vegetation memory. Vegetation memory describes the effect of antecedent environmental and ecological conditions on the present ecosystem state. Ogle et al. (2015) expanded on this definition by identifying the following three important characteristics of vegetation memory (Ogle et al., 2015): (1) memory length—the extent of time through which past conditions significantly affect the current state of vegetation; (2) memory strength—the magnitude of the effect that past events/conditions have on the current state of vegetation and (3) temporal patterns—the variation in relative impacts of antecedent conditions at different points in time. Here, we investigate memory length and memory strength aspects. Note that under this framework, vegetation memory does not quantify vegetation response to explicitly considered perturbation events, but instead aims to identify the effects of cumulative environmental conditions on vegetation (Kannenberg et al., 2020).

Additionally, vegetation memory can occur as a result of both 'intrinsic' (e.g. internal vegetation dynamics affecting the recovery rate) and 'extrinsic' forcing (e.g. a lagged response to climate variables) (Ogle et al., 2015). Indeed, it has been suggested that the strength of the intrinsic vegetation memory, identified using an autoregressive model in which the previous time step's vegetation metric is used as a predictor alongside current climate variables (e.g. temperature, precipitation), can be used as an indicator for the recovery rate (i.e. engineering resilience). Because ecological theory indicates that increased autocorrelation occurs in models in which an ecological state variable is increasingly placed under stress and approaching a threshold (Scheffer et al., 2009), reduced recovery rate (i.e. a stronger intrinsic memory as indicated by an increased autoregressive coefficient) may be a proxy of reduced resilience. Indeed, although one study has extended such analyses to investigate the changing strength of autocorrelation signals along individual time series (e.g. Liu et al., 2019), the most common approach in remote-sensing analysis has been to use a space-for-time approach, in which the autocorrelation of the time series is incorporated into some kind of model at the level of the individual pixel to assess changing patterns of resilience across a region, for example, in tropical forests (Papagiannopoulou et al., 2017; Verbesselt et al., 2016), Mediterranean forests (Gazol et al., 2018) and global drylands (De Keersmaecker et al., 2015).

However, although theoretical simulations may predict reduced recovery rates as a result of reduced ecosystem resilience, it is unclear if the simple approximation of using the first-order autoregression (AR1) coefficient can be universally applied at a global scale. While the AR1 coefficient may be applicable for identifying engineering resilience in some settings, this relies on the assumption that all other extrinsic variables have been accounted for. If not, then the autocorrelation coefficient used to identify intrinsic memory has the potential to mask the effect of other extrinsic forcing variables. For example, one recent study showed that some regions that exhibited high memory-effect coefficients in previous studies could be better explained by varying the length of extrinsic memory (Liu et al., 2018). As a result, the underlying applicability of this metric as proxy for ecological resilience must be considered before it can be implemented more broadly.

One region of particular relevance for such studies are global drylands. Global drylands, defined as areas in which crop production is limited by water availability (Adeel et al., 2005; Millennium Ecosystem Assessment, 2005b), are commonly observed to exhibit strong intrinsic memory coefficients, and are therefore assumed to exhibit low engineering resilience (De Keersmaecker et al., 2015). Additionally, these systems function as important carbon pools (Tian et al., 2017) and may be prone to locally facilitated regime shifts (Xu et al., 2015). Thus, bolstering the ecosystem resilience of these regions is essential in securing the reliability of agricultural landscapes for local and global communities.

Here, we investigate the factors influencing vegetation memory in global dryland regions. Specifically, we combine a state-of-the-art climate reanalysis product and satellite-based global vegetation indices to extend previous analyses of vegetation memory in drylands in terms of (1) spatial and temporal coverage, (2) consistency,

(3) accuracy and (4) climatological variables at a global scale. Specifically, we investigate (i) the relative importance of extrinsic factors and intrinsic-vegetation memory for determining the vegetation response in dryland regions; (ii) the length of extrinsic memory (i.e. the time period in which past external factors influence the current system state) and (iii) the strength of this memory (i.e. the magnitude of the vegetation memory coefficients and whether this coefficient is positive or negative). Using this information, we then consider our findings in the context of understanding patterns of ecological resilience worldwide and investigate capability of distinguishing extrinsic from intrinsic vegetation memory.

2 | MATERIALS AND METHODS

Dryland regions were identified following the Millennium Ecosystem Assessment (Millennium Ecosystem Assessment, 2005b) which classifies any region as a dryland which exhibits aridity index (long-term mean ratio of mean annual precipitation to mean annual evapotranspiration) values below 0.65 (Millennium Ecosystem Assessment, 2005a).

2.1 | Datasets

We used GIMMS NDVI 3g data to identify vegetation response in global dryland regions between January 1982 and December 2015. NDVI is a compound vegetation index made up from reflectance in the red and near-infrared reflectance bands. It is highly correlated with vegetation cover (Harris et al., 2014; Tian et al., 2017), productivity (Gamon et al., 1995) and photosynthetic performance (Gamon et al., 1995; Pettorelli et al., 2005). The GIMMS dataset provides bi-weekly (Stow et al., 2004) NDVI snapshots on a 0.083°×0.083° (Liu et al., 2018) (~9.27 km×9.27 km) resolution at global scale. We subsequently built monthly maximum composites to minimise the impacts of cloudy periods (Stow et al., 2004). While NDVI records tend to saturate in regions of high biomass and thus high NDVI values (Huete et al., 2002), these issues are unlikely to affect dryland regions.

For independent climate data, we used the European Centre for Medium-range Weather Forecast's (ECMWF's) ReAnalysis 5 (ERA5) (Balsamo et al., 2015; ECMWF, 2018a). ERA5 is created using the ECMWF's integrated forecasting system and a large volume of satellite and ground-based data from a wide variety of data providers through the use of data assimilation (ECMWF, 2018b). ERA5 benefits from recent methodological advancements in data assimilation, incorporating a wide range and high volume of weather station observations and improved understanding of physical processes within the integrated-forecasting system (ECMWF, 2018b, 2018c). It has been demonstrated to outperform independent satellite observations over land (Tang et al., 2021) and marks a substantial improvement over previous reanalyses (Martens et al., 2020; Tarek et al., 2020).

One major advantage of using climate reanalysis products to understand vegetation memory is that they enable the study of responses at higher temporal resolution and consistency than previous studies. For example, the CRU3.0 dataset is less well suited for dryland regions because it contains large areas of the globe where precipitation time-series data must be replaced with mean values (Macias-Fauria et al., 2014), resulting in large areas of missing data when such regions are masked out (Liu et al., 2018). Reanalysis products have been widely used to shed light on physical processes (ECMWF, 2018d; Tarek et al., 2020) which are highly influential in determining vegetation memory properties. For our analyses, we selected two main ecosystem drivers: soil moisture and air temperature.

Soil Moisture (Qsoil) was used as a proxy of local water regimes given that water-dependent vegetation memory is likely to rely on water availability to root systems (Ogle et al., 2015). Qsoil metrics were included to take into account that precipitation events may be subject to further soil processes such as pore connectivity for precipitated water to be available to plant roots (Smith et al., 2017). Therefore, we anticipated that soil moisture would serve as a more direct proxy of local water regimes compared to the drought indices used in previous studies.

ERA5 includes four distinct layers in the soil for the calculation of Qsoil indices: (1) Soil Moisture (0–7 cm) (Qsoil1), (2) Soil Moisture (7–28 cm) (Qsoil2), (3) Soil Moisture (28–100 cm) (Qsoil3) and (4) Soil Moisture (100–255 cm) (Qsoil4). Typical drought indices (e.g. SPEI) do not allow for this additional distinction. Within ERA5, unfrozen ground water ($\bar{\theta}$) across all four soil layers (k) is defined as:

$$\bar{\theta} = \sum_{k=1}^{4} \left(R_k \times \max\left[f_{liq;k} \theta_k, \theta_{pwp} \right] \right) \tag{1}$$

with R_k being the root fraction of soil layer k which is a fixed metric according to Land-Cover Classification Systems (LCCSs), and the statement $\max\left[f_{liq;k} \theta_k, \theta_{pwp} \right]$ calculating the amount of unfrozen soil water in soil layer k. $f_{liq;k}$ is a parametrised function of soil temperature; θ_{pwp} denotes the permanent wilting point according to soil texture. For a more in-depth explanation of how Qsoil is calculated within ERA5, see the IFS Documentation CY45R1 Chapter 4 Physical Processes (ECMWF, 2018d).

Air Temperature was used as an additional predictor in this study given its links to vegetation sensitivity (Seddon et al., 2016), tree-ring growth (Esper et al., 2015) and global primary production (Prince & Goward, 1995), in addition to severe drought events with possible large consequences to local vegetation (Allen et al., 2010). Within this study, we used Air Temperature (at 2 m above ground) (Tair) as contained within the ERA5 dataset, due to the demonstrated impact of Tair on different aspects of plant physiology and plant morphology which may manifest in vegetation memory.

ERA5 data are available for hourly intervals (which we averaged to monthly means) from 1950 to present day at a 30 km×30 km spatial resolution of global coverage making the resolution of ERA5 and AVHRR-based GIMMS NDVI 3g incompatible. We resolved this issue by statistically downscaling ERA5 data using kriging (see

Supporting Information: 'Statistical Downscaling'). Upon publication of ERA5-Land climate reanalysis (Sabater, 2021) data at 9 km × 9 km spatial resolution (which matches the resolution of the NDVI data), we also used this higher-resolution dataset to compare results (see Supporting Information: 'ERA5-Land Results'). Using native ERA5-Land data in our analyses made virtually no change to the estimated vegetation-memory model coefficients. Consequently, we present here our vegetation-memory coefficients obtained via downscaled ERA5 data since our analyses proved to be robust to the downscaling implementation.

Methodology used here to obtain ERA5(-Land) data and statistical interpolation thereof has been made available by Kusch and Davy (2022).

2.2 | Statistical approach

We extracted data for each variable (NDVI, Tair, Qsoil) and used linear detrending to avoid effects of changing abiotic conditions over long time-series (De Keersmaecker et al., 2015). Note that recent work by Verbesselt et al. (2016) tested several methods for detrending time series to identify autocorrelation components, including methods accounted for varying seasonality and nonlinear trends. They showed that different detrending methodology of remote sensing data may lead to qualitatively similar results with highly flexible methods outperforming others in settings of time-varying amplitude/phase of time series. To ensure robustness of our model algorithm to the effect of different detrending approaches, we executed additive and multiplicative detrending for a representative, latitudinally stratified sample across the totality of our study region. While estimates of vegetation memory model components did change numerically respective to detrending methods, their interpretation as we present it in the following remained unaltered for each detrending method used (see Supporting Information: 'Detrending Comparison').

Following detrending, we standardised the NDVI time series to z-scores to obtain deviations of monthly means/monthly anomalies (De Keersmaecker et al., 2015):

$$Anomaly_i = \frac{Detrended_i - \overline{Detrended_{month}}}{SD_{Detrended,month}} \quad (2)$$

with i indexing individual, detrended data records. This resulted in a final set of monthly time series of vegetation dynamics expressed as divergences from seasonal trends across the study regions. Lagged effects were calculated as (1) $NDVI_{t-1}$ (to identify intrinsic vegetation memory) using z-score NDVI data and (2) cumulative lags of detrended $Qsoil/Tair$ data (to identify extrinsic Qsoil/Tair-driven memory) with lags ranging from 0 (instantaneous effects) to annual effects (aggregated over 12 months of detrended Qsoil/Tair records) in steps of 1 month at a time. These cumulative lag values are subsequently standardised to z-scores using the same approach as shown in Equation 2.

To assess the relative importance of intrinsic memory and extrinsic climate forcing, we used a linear modelling approach (e.g. De Keersmaecker et al., 2015). Our vegetation-memory models are based on the following specification:

$$NDVI_t = \beta_0 + \beta_{t-1} \times NDVI_{t-1} + \beta_{Qsoil} \times Qsoil_{k;m} + \beta_{Tair} \times Tair_n \quad (3)$$

with $NDVI_t$ and the Autoregressive NDVI Coefficient ($NDVI_{t-1}$) being standardised NDVI anomalies at time step t and $t-1$, respectively; $Qsoil_{k;m}$ denoting Qsoil data at depth level k (translating to Qsoil1–Qsoil4) and cumulative lag values of lag m, and $Tair_n$ denoting Tair data as the cumulative lag values of lag n. As such, Equation 3 represents a model framework in which models were run for all unique combinations of m and n but never considering multiple values of either m or n in the same model.

We used Principal Component Analysis (PCA) regression to limit the effects of collinearity in our predictor variables. Subsequently, we performed model selection to identify the cumulative soil moisture and air temperature lags which present the most explanatory power through comparison of the model Akaike Information Criterion (AIC) values (lowest AIC indicates best model performance). The regression coefficients from the PCA regression were then back-transformed to represent PCA input-variable effects (see formula 1) using PCA loadings and PCA model coefficient (see Supporting Information: 'Model Workflow and Interpretation'). This results in a proxy of Qsoil- and Tair-memory length of local vegetation.

2.2.1 | Model comparisons

To reduce computational requirements in the downscaling process (i.e. downscaling all four Qsoil levels for our pre-selected study regions and only the most biologically important Qsoil layer globally), we employed model comparison to determine which soil moisture layer has the greatest influence on vegetation anomalies. To do so, we executed the models specified in Equation 3 with k (Qsoil layer) ranging from 1 to 4, m (Qsoil lag length) ranging from 0 to 12 and n (Tair lag length) fixed to 0 in an effort to reduce computational demand. We then compared the absolute values of soil moisture coefficients (β_{Qsoil}) across all pixels within each model output using Mann–Whitney U-tests for a set of five pre-selected study regions (i.e. South-Eastern Europe, the Caatinga [N-E Brazil], Australia, the contiguous US and the Sahel region) which exhibited marked patterns of strong vegetation memory in contemporary studies (De Keersmaecker et al., 2015, 2017; Liu et al., 2018; Seddon et al., 2016; Vicente-Serrano et al., 2013). Across all pre-selected study regions (South-West Europe, Australia, Caatinga, the contiguous US and the Sahel region), $Qsoil1$ (soil moisture in a band of 0–7 cm depth) was identified as the most meaningful out of all the soil moisture variables. Therefore, we carried out the global analysis using only $Qsoil1$ input out of the four available soil moisture parameters within ERA5.

2.2.2 | Variance partitioning

To assess the relative importance of intrinsic and extrinsic vegetation memory components in driving the system's response to disturbances, we used variance partitioning on each pixel in our study. In this procedure, we determined the relative importance contained in the vegetation memory model predictors $NDVI_{t-1}$ (intrinsic memory), $Qsoil_{k;m}$ (extrinsic soil moisture memory of layer k and cumulative lag m) and $Tair_n$ (extrinsic air temperature memory at cumulative lag n) using a partial regression approach (see Supporting Information: 'Variance Partitioning'). This allowed us to map the relative importance of components of vegetation memory, and spatial inspection of which variables best explain NDVI anomalies.

3 | RESULTS

3.1 | Vegetation-memory properties

According to R^2 scores, our vegetation-memory models performed best across parts of Saudi-Arabia, around the Gulf of Mexico, the Caatinga, South Africa, the Horn of Africa, parts of Argentina, Morocco and northern Algeria, and Australia (see Figure 1).

The highest intrinsic vegetation memory coefficients (i.e. β_{t-1}, intrinsic memory strength) were found across Australia, South Africa, Texas, and Algeria/Morocco and weakest across the Sahara Desert, and the Russian steppe (see Figure 2a). The patterns of intrinsic vegetation memory strength (Figure 2a) are mostly mirrored by the strength in the extrinsic vegetation memory linked to soil moisture (β_{Qsoil}, Figure 2b). Strong positive effects of soil moisture are most prevalent across Australia, South Africa, west of the Gulf of Mexico, the Horn of Africa and the Caatinga. However, extrinsic soil-moisture memory

coefficients were negative in some areas, typically in areas of low intrinsic-vegetation memory such as the northern regions of drylands in the Russian steppe, the Sahara desert, north-eastern China, south Saudi-Arabia and parts of the south-western contiguous United States.

In addition to variations in extrinsic soil-moisture memory strength, we also observed variations in the length of extrinsic soil-moisture memory worldwide (as exemplified by lag length, m, see Figure 3a). These values range from fast-responding vegetation (i.e. soil-moisture memory length close to 0 months) to regions of slow response (i.e. soil-moisture memory length close to 12 months). While clear global patterns of soil-moisture memory lags are difficult to establish, we did find a clear west–east gradient of soil-moisture-memory length across both Australia and North America. Additionally, soil-moisture-memory length in Eurasia and Africa increases from north to south. Finally, areas of negative soil-moisture-memory strength are almost exclusively characterised by soil-moisture-memory lags of zero months (i.e. instantaneous responses).

Air-temperature-memory coefficients (β_{Tair}, extrinsic memory strength) show large, negative effects across many dryland regions (i.e. dryland vegetation performance is diminished by warmer temperatures) including South Africa, the Caatinga, parts of Australia and Kazakhstan (Figure 2c). However, there are also areas with positive air-temperature-memory coefficients, across Algeria, parts of the Mongolian steppe, parts of Australia as well as Polish and Turkish drylands. The patterns related to the length of the air-temperature-memory tend to be highly localised (n, see Figure 3b).

### 3.2 | Relative importance of vegetation-memory components

Although there are clear spatial patterns in the different components of vegetation memory, in general, the relative strength of the intrinsic
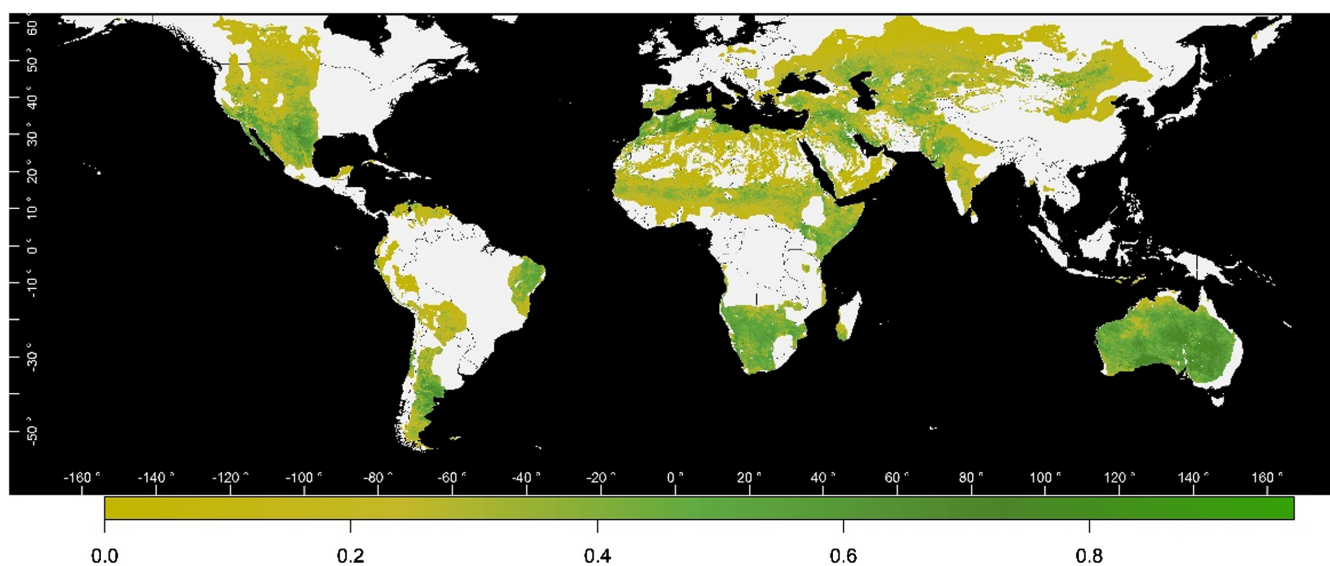
FIGURE 1 Adjusted R^2 of the final models: coefficient of determination of final models following model selection among the set of candidate models established by Equation 3 (with soil layer k fixed at 1). The final model per pixel is hereafter used to report vegetation memory coefficients for global drylands worldwide
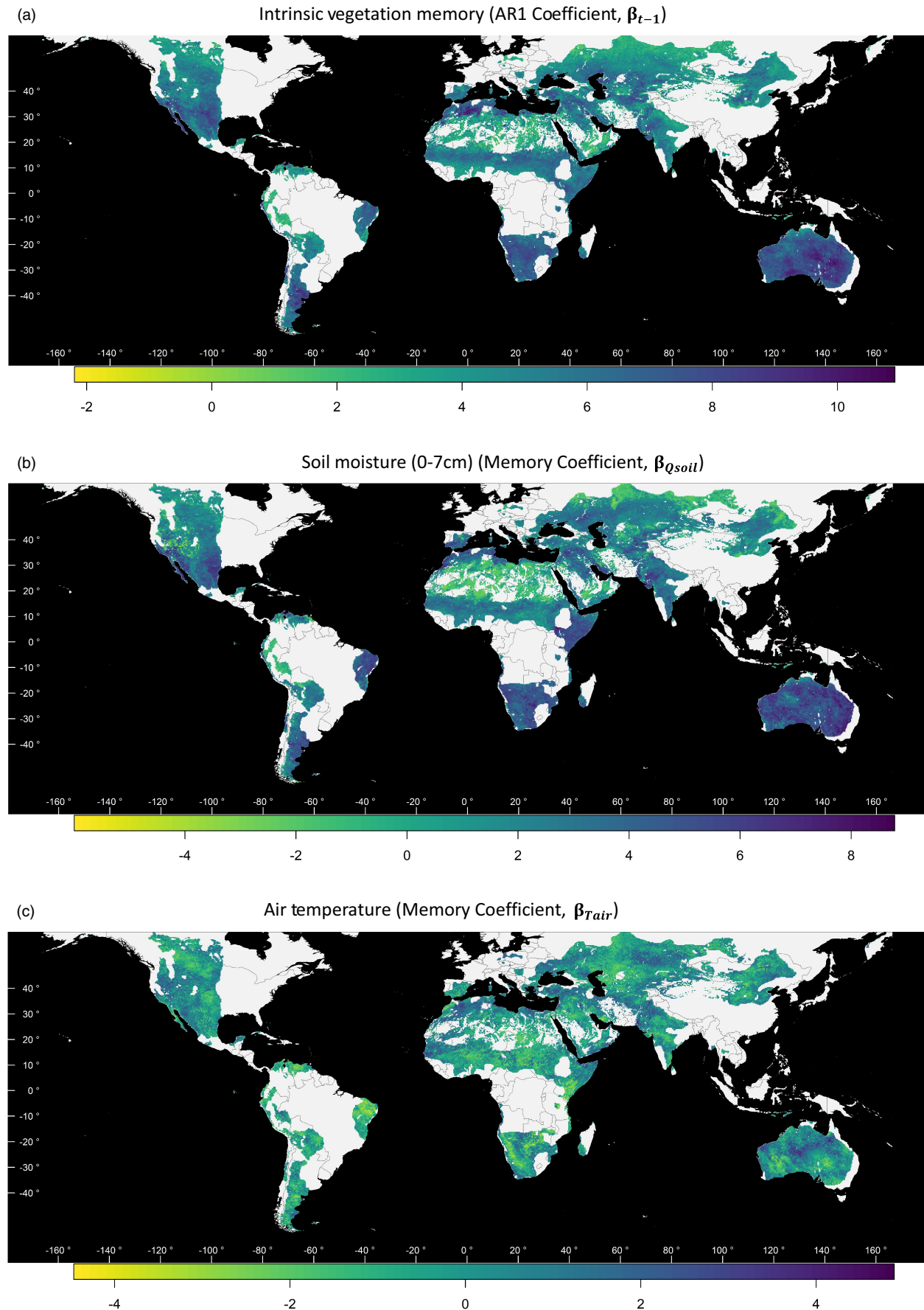
FIGURE 2 Vegetation memory strength: Vegetation memory strength for (a) intrinsic memory (β_{t-1}); (b) extrinsic soil moisture memory (β_{Qsoil}), and (c) extrinsic air temperature memory (β_{Tair}). Note that negative values for intrinsic vegetation memory signify negative autocorrelation of z-score ndvi values. See Table S1 in Supporting Information for coefficient interpretations

(a)

Soil moisture (0-7cm) (Lag Length, m)

(b)

Air temperature (Lag Length, n)
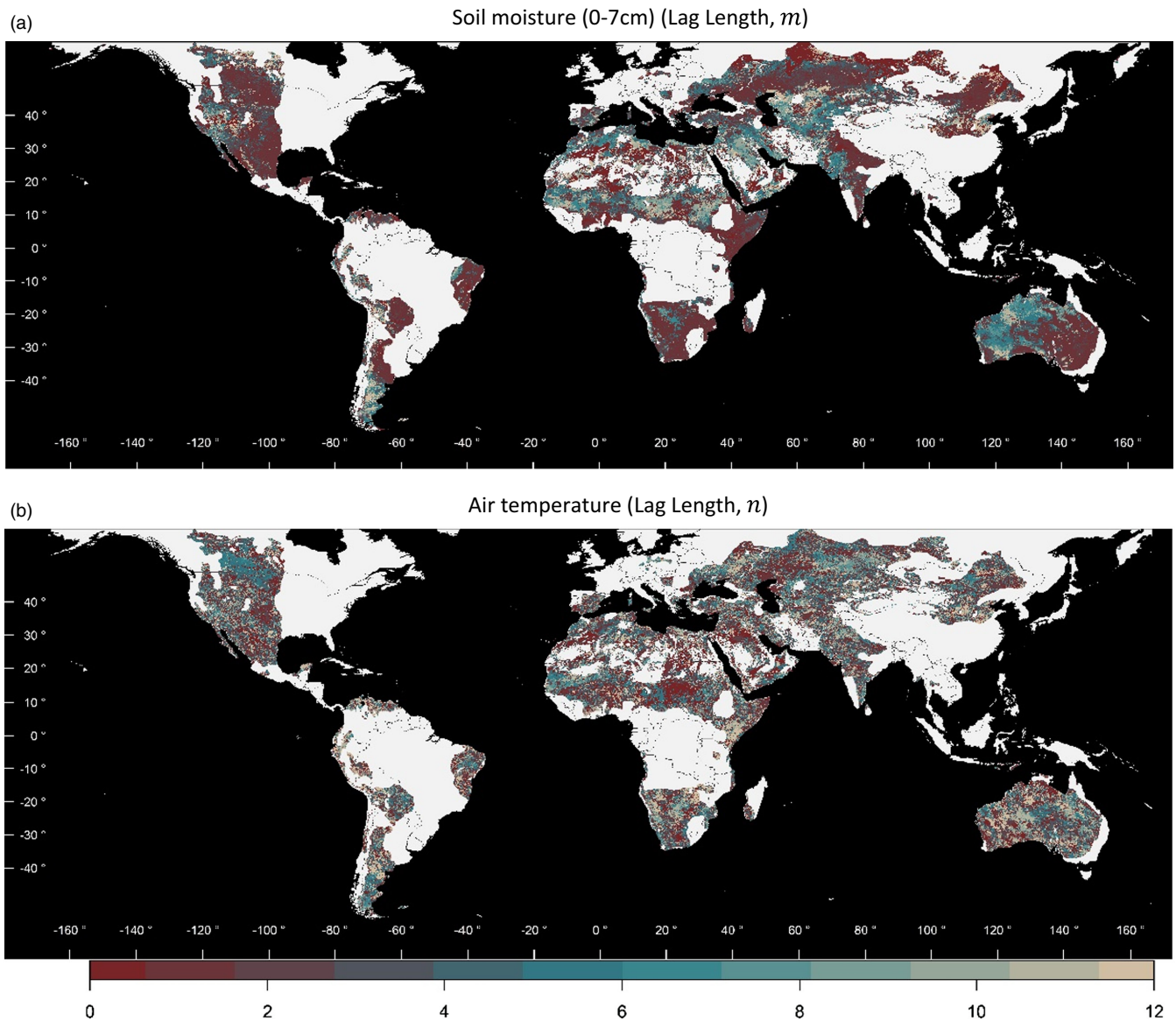
FIGURE 3 Vegetation memory length: Vegetation memory length for (a) extrinsic soil moisture memory (**m**), and (b) extrinsic air temperature memory (**n**). Note that colour palette between all have been synchronised to make the outputs of regions comparable

FIGURE 4 Vegetation-memory strength magnitude: Relative strength of the three vegetation memory coefficients (β_{t-1}, β_{Qsoil}, β_{Tair}) as determined by the absolute values of the model coefficients in Equation 3 and visualised in Figure 2
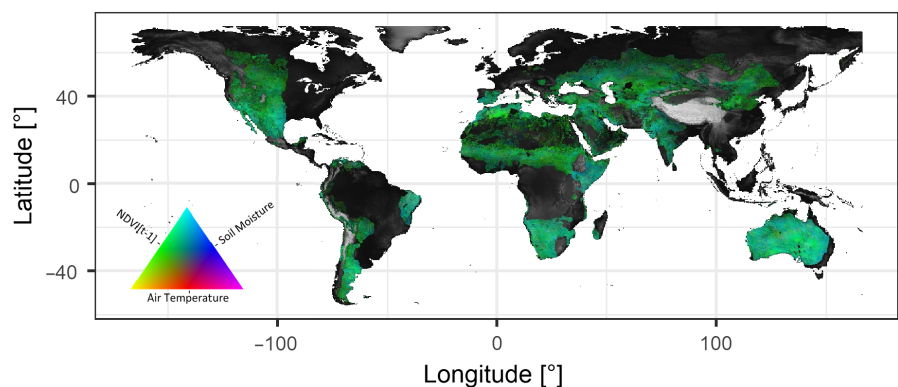
memory coefficient (β_{t-1}) is much greater than either of the extrinsic memory coefficients (β_{Qsoil} and β_{Tair}). Overall, model coefficients are largest for intrinsic vegetation memory (β_{t-1}), followed by soil-moisture memory (β_{Qsoil}), then air-temperature memory (β_{Tair}) thus identifying a hierarchy of importance of these parameters in shaping the vegetation performance/NDVI values of local dryland vegetation through time and space (Figure 4). Here, intrinsic vegetation memory and soil-moisture effects control most of the global dryland vegetation performance.

Similarly, although patterns of intrinsic and extrinsic vegetation-memory strength are strikingly analogous in terms of their spatial patterns (see Figure 2), variance partitioning indicates most of the information is contained within intrinsic vegetation memory ($NDVI_{t-1}$), with the coefficient representing $Qsoil1$ memory (and shared information between the two variables) constituting almost all of the remaining explained variance in the models (Figure 5).

As such, almost all explanatory power of our vegetation-memory models is contained within $NDVI_{t-1}$ and Qsoil1 data. However, the comparatively high values of variance shared between these two variables show the difficulties in distinguishing intrinsic from extrinsic vegetation memory. This is also confirmed by the clear overlap of spatial patterns (Figure 2).

4 | DISCUSSION

Our approach builds on previous studies which have identified components of vegetation memory using satellite data (e.g. De Keersmaecker et al., 2015; Liu et al., 2018; Seddon et al., 2016; Vicente-Serrano et al., 2013), using climate reanalysis data (ERA5 using statistical downscaling). In addition, we attempted to isolate the intrinsic- and extrinsic-memory effects for global drylands worldwide and found similar overall results when higher resolution mechanistic downscaling was used (see Supporting Information).

4.1 | Patterns of vegetation memory in global drylands

One key observation from this study is that the $NDVI_{t-1}$ coefficient (β_{t-1}) dominates in terms of the variance explained in our models across large parts of the Earth's surface. This result occurred in spite of the fact that our models incorporated the use of climate reanalysis

data. One interpretation from these results is that, overall, global dryland regions are characterised by strong intrinsic vegetation memory, and that this effect is—in general—much stronger than any extrinsic memory identified as a result of ERA5 soil moisture or temperature variability (Figures 4 and 5).

A second key finding of our study is represented by the strength of extrinsic vegetation memory (coefficients β_{Qsoil} and β_{Tair}) which varies considerably across regions, although never reaching the same magnitude as the intrinsic $NDVI_{t-1}$ coefficient. We found that soil-moisture memory exerts a much greater effect on dryland vegetation than air temperature, with global dryland vegetation broadly responding as would be expected: positively to wetter conditions (i.e. positive β_{Qsoil}) and negatively to neutral to elevated air temperatures.

Counterintuitively, our study identified several areas in which positive soil-moisture anomalies lead to a decrease in vegetation productivity (negative NDVI anomalies) captured in negative values of β_{Qsoil}. These effects coincide with response times (m) of 1 month and faster. One possible explanation for this finding is that positive soil-moisture anomalies in these regions, coupled with severe downpour and flooding events, can lead to a decrease in vegetation performance in certain vegetation communities (Broich et al., 2018). Note, however, that the negative coefficients of soil-moisture memory are far smaller in extent and magnitude than their positive counterparts. Additionally, our analysis revealed that global dryland vegetation performance can react to positive air temperature anomalies in one of two ways: (1) negatively at different time lags or (2) positively at long time lags captured as negative and positive values β_{Tair}, respectively. This may be indicative of different physiological strategies and capabilities of dealing with increased heat-stress (Wang et al., 2016). This result may also reflect lower data quality during rainfall events, with cloudiness screening images during higher rainfall events. However, dryland regions tend to exhibit low cloudiness and cloudiness has been demonstrated to not bias the monthly NDVI product (Calvet & Barbu, 2015). Note that our models
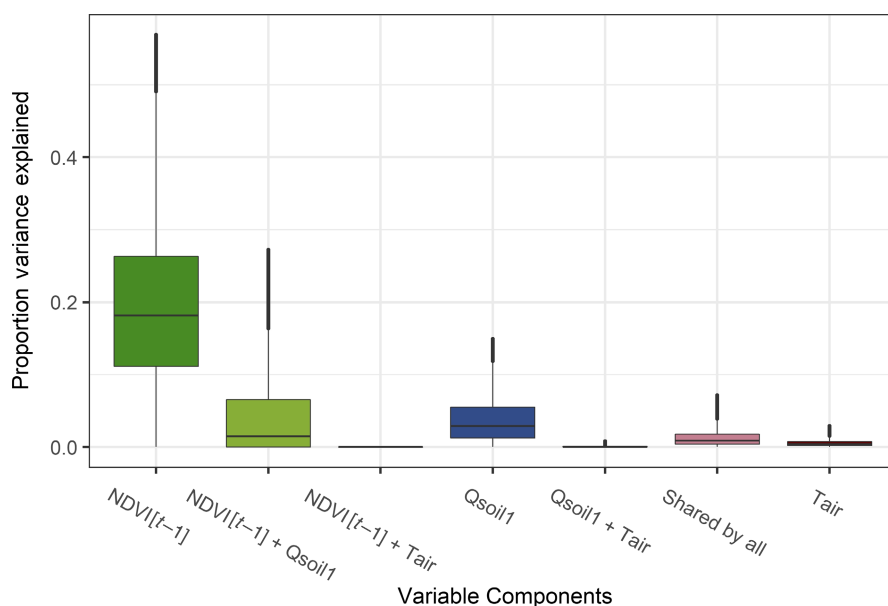
FIGURE 5 Vegetation memory variance partitioning: Variance in anomalies of NDVI explained by model parameter across global dryland raster cells. Variances portrayed here have been limited to 95% quantiles of their respective ranges. Solid bars beyond boxplot whiskers represent outlier data points beyond the 95% range depicted by the boxplot and whiskers (McGill et al., 1978; Wickham, 2016)

did not differentiate between memory during different seasons thus potentially suffering from masking of the strength of the memory coefficients with opposing signs (Wen et al., 2019). Future vegetation memory model development may benefit from including interseasonal distinction of memory worldwide.

Patterns of extrinsic-memory length (*m* and *n*) also vary considerably within and between regions. One example of this is the east–west gradient in soil-moisture memory length (*m*) across Australia, with shorter responses in the east and longer responses in the west. Other regions exerting short vegetation memory to soil-moisture anomalies are located in south and east Africa as well as the Caatinga and parts of Argentina, while longer soil-moisture memory is especially present throughout the Sahel region. Similar to extrinsic-memory strength, these patterns are likely a consequence factors including (but not limited to) (1) local antecedent disturbance regimes (Yin et al., 2015), (2) plant function (Nielsen et al., 2019), (3) life-history strategies (Adler et al., 2014; Archibald et al., 2019) and (4) soil properties (Smith et al., 2017; Wan et al., 2016).

To investigate the effect of different life-history strategies and plant functional types on vegetation memory components, we investigated the west-to-east gradients of extrinsic soil moisture memory lags across Australia (see Figures 3b and 7). The drylands across Australia as defined by the Sustainable Development goals (Sustainable Development Goals, 2020) include forest and grassland (World Wildlife Fund, 2020). Previous work using tree-ring data indicates that cumulative antecedent conditions contribute to changes in tree resistance and recovery (Lloret et al., 2011). Indeed, at least some of the variation in patterns of the soil-moisture memory lag can be explained by major differences in land-cover between forests and grasslands. For example, we extracted values of soil-moisture memory lags (*m*) across Australia and assigned them either to a forest or grassland category based on an ecoregion mask (World Wildlife Fund, 2020) (Figure 6).

Forest soil moisture memory lags do indeed show a higher proportion of samples with a lag of 2 and 12 months (the maximum cumulative lag length allowed in our model framework) which indicates a longer response time in forest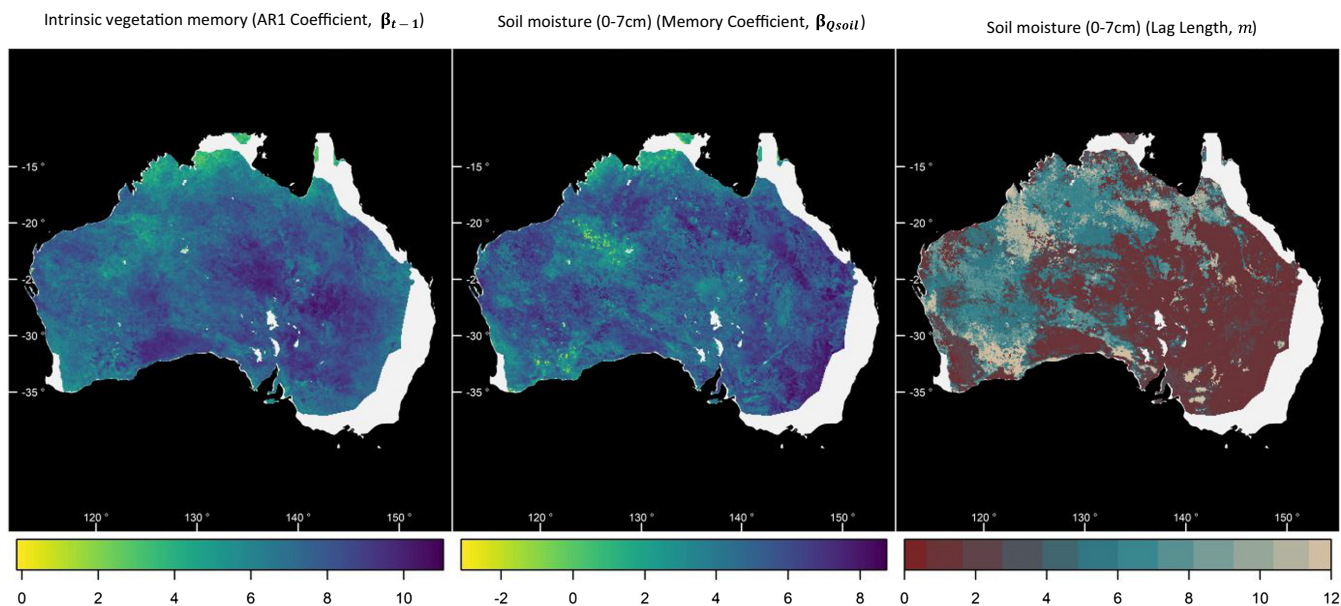 ecosystems than in grasslands where such a spike is absent. However, both forest and grasslands also respond to cumulative soil moisture pressures at time-frames smaller than 3 months. Further studies of these regions at higher spatial resolutions which meaningfully link vegetation-plot data to remotely sensed data are needed to uncover the underlying processes that enable the overall patterns in vegetation memory we have observed.

Vegetation-memory patterns may additionally be affected by anthropogenic influence on the vegetation response. For example, Abel et al. (2021) estimated trends in vegetation-rainfall sensitivity (inferred from calculating a moving-window relationship between NDVI and globally gridded precipitation data for the past 15 years) in global drylands and showed that negative trends in this relationship were best explained population changes (estimated from modelled census data in 2010, extrapolated and then interpolated between 2000 and 2015). In contrast, positive trends in this relationship were best explained by a combination of changing climatic conditions, and by the intensification and expansion of human land management. Since our study incorporated the use of monthly vegetation and climate time series, it was not possible to incorporate such effects in our approach. Accounting for such anthropogenic effects ought to be a priority moving into future studies.

Furthermore, our vegetation memory modelling framework does not account for nonlinear relationships between NDVI time-series and environmental conditions (e.g. soil moisture and air temperature). Previous work focussing on tropical rainforests, however, has demonstrated that temporal autocorrelation of NDVI time series (i.e. intrinsic vegetation memory) is affected by environmental conditions (Verbesselt et al., 2016). Therefore, we expect that future research on vegetation memory may benefit greatly from the adoption nonlinear modelling techniques as has been used for understanding climate vegetation dynamics previously by Papagiannopoulou et al. (2017). Such consideration for changes in temporal autocorrelation on NDVI time series may be further enhanced by explicitly accounting for spatial autocorrelation in vegetation dynamics so as to identify regions exhibiting critical slowing down of recovery rates with more certainty (Scheffer et al., 2015; Xu et al., 2015).
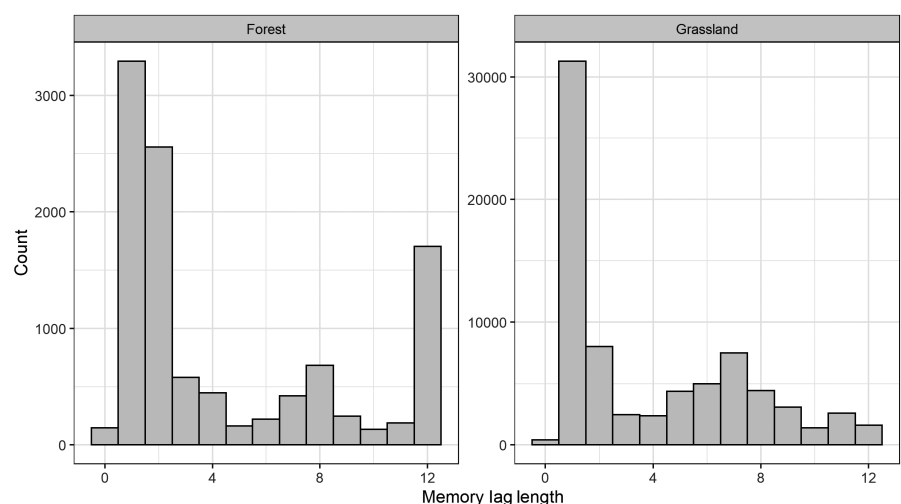
FIGURE 6 Soil moisture memory length across australia: Comparison of soil moisture memory lag (*m* in Equation 3) for grassland and forest regions across Australia. The spatial gradient of the soil moisture memory lag reported here is shown in Figure 7

Intrinsic vegetation memory (AR1 Coefficient, β_{t-1})   Soil moisture (0-7cm) (Memory Coefficient, β_{Qsoil})   Soil moisture (0-7cm) (Lag Length, m)

FIGURE 7 Patterns of vegetation memory components across Australia: Comparison of vegetation memory model components across Australia. Our study shows homogeneous $NDVI_{t-1}$ and diffuse extrinsic soil-moisture vegetation-memory patterns as well as a clear west-to-east gradient in soil-moisture-memory length which matches the west-to-east gradients of intrinsic vegetation memory by Seddon et al. (2016) and De Keersmaecker et al. (2015)—see figure S3 in Seddon et al., 2016 and figure 1b in De Keersmaecker et al. (2015)

4.2 | The use of ERA5 data in vegetation response studies

One major advantage of using climate reanalysis products to understand vegetation memory is that they enable the study of responses across temporal periods of finer resolution and with a greater spatial coverage compared to previous studies. For example, Liu et al. (2018) used the CRU3.0 dataset, which provides a gridded dataset based on global weather station data for air temperature, precipitation and solar radiation. However, because large areas of the Earth's surface do not contain weather stations providing consistent time series, many areas (particularly in tropical regions), in many cases, precipitation values are replaced with climatological mean values (Macias-Fauria et al., 2014). This is a problem for analyses based on understanding patterns ecological resilience in dryland regions, since the vegetation response to climate variability is likely to be an important component, and a consequence of this is that large areas of the Earth's surface are required to be masked from any analysis. The ERA5 data allowed to us to provide an assessment of three vegetation-memory components for dryland ecosystems worldwide without encountering these issues of temporal gaps in the data (ECMWF, 2018d). In this analysis, we used ERA5 data which was statistically downscaled to match the NDVI resolution. Indeed, comparison of the results with more recent ERA5-Land data based on dynamic models shows similar results and demonstrates the capabilities of both approaches moving forward.

A second advantage is that the ERA5 data enabled us to incorporate the use of soil moisture as a bioclimatic variable to reflect water availability in dryland regions. Our expectation was that soil moisture would be a better predictor than, for example, the weather station inferred SPEI drought index because 1–3 month lagged precipitation indices have been shown to be a predictor of vegetation productivity in dryland regions as a result of soil infiltration processes. Since soil moisture availability would represent a more direct indicator of the water available to the plant, we expected this to be a strong predictor in dryland regions.

However, despite the incorporation of soil moisture data in our analysis, the autoregressive parameter (i.e. the indicator of intrinsic memory) remained the strongest predictor across large areas of the Earth's surface, and in some cases the relative strength of the coefficient for soil moisture was actually less than that when drought indices have been used (e.g. De Keersmaecker et al., 2015). Furthermore, the patterns of soil-moisture memory lags we identified do not coincide with the precipitation-driven memory lag identified by Liu et al. (2018) or the SPEI-informed memory lag by Vicente-Serrano et al. (2013). Such variations in the results between studies suggest that ground-based validation is required to understand better the differences in these approaches of the different datasets, and to determine whether ERA5 data provide a useful tool for future research for assessing global patterns in vegetation dynamics in response to climate variability.

4.3 | The use of intrinsic memory as an indicator of engineering resilience

Intrinsic vegetation memory, usually identified as autoregressive coefficients of vegetation indices (e.g. Seddon et al., 2016), has been used as an indicator of vegetation engineering resilience (i.e. recovery speed) (De Keersmaecker et al., 2015; Liu et al., 2018). Our

analysis, which involved using ERA5 data to assess the factors influencing vegetation memory in global drylands, reveals some important caveats to this assumption for two main reasons.

First, the spatial patterns demonstrating the relative strength of the autoregressive parameter (i.e. intrinsic vegetation memory e.g. $NDVI_{t-1}$) vary considerably across the various studies which have quantified the value of intrinsic vegetation memory relative to different extrinsic vegetation-memory variables. For example, our results revealed relatively high levels of intrinsic vegetation memory across Australia, a weak west-to-east gradient of increasing correlation between NDVI anomalies and soil moisture anomalies, and a strong west-to-east gradient of response time to soil-moisture anomalies (see Figure 6). These results are similar to Liu et al. (2018), but are in contrast to those by Seddon et al. (2016) and De Keersmaecker et al. (2015), who identified a clear west-to-east gradient of intrinsic vegetation memory (AR1 coefficient) and extrinsic drought-driven memory, respectively. While the overall model specifications are similar across these three studies, the main differences are in the choice of datasets used to represent extrinsic forcing. For example, Liu et al. (2018, figure 2a–c) showed how varying the length of the extrinsic lags could compensate for some of the variance explained by an AR1 only model, while Seddon et al. (2016) and De Keersmaecker et al. (2015) used a combination of satellite-derived vegetation and water availability/drought indices calculated from two different sources and which did not account for variable time lags (see Figure S3, Seddon et al., 2016, Extended Data Figure 1b, De Keersmaecker et al., 2015). Similar findings are observed across the Caatinga region in NE Brazil. Here, Seddon et al. (2016) found relatively low intrinsic memory compared to the response in water availability, while our study and De Keersmaecker et al. (2015) found intrinsic memory to have a higher overall importance than soil moisture in this region. It stands to reason that implementation of uncertainty metrics for lag selection could further change these landscape-scale vegetation memory gradients.

Nevertheless, these examples indicate an important caveat with regards to interpreting spatial patterns in the $NDVI_{t-1}$ coefficient across different analyses, namely, that the relative importance of this variable in any model will vary strongly depending on the input variables used. As a result, interpretations of components of vegetation resistance and recovery at large spatial scales may be highly sensitive to the original forcing variables used. For example, in previous studies, eastern Australia and the Caatinga have been interpreted as being resistant to precipitation anomalies, while the high autocorrelation coefficient in western Australia may be interpreted as having an overall lower vegetation resilience (e.g. De Keersmaecker et al., 2015). In our study, the west–east gradient in this autoregressive parameter does not exist to the same extent, and different interpretations arise from the inclusion of slightly different variables.

This issue is further compounded by temporal aggregations of input variables. By enabling the selection of the optimum soil-moisture memory-length (i.e. between 0 and 12 months), our

model had a more flexible approach to the identification of the strength of an extrinsic forcing variable compared to those using only a fixed time window. This increase in model flexibility may also have resulted in different patterns of intrinsic memory being observed. In the Australia example, a west–east gradient is observed in extrinsic memory length to soil moisture anomalies in our study (Figure 7, right panel), a pattern which resembles the west–east gradient in *intrinsic* memory identified by Seddon et al. (2016) and De Keersmaecker et al. (2015). Thus, again, these results suggest a compensation effect of the AR1 coefficient in model when a fixed (e.g. 1- or 3-month lag) vs. flexible (i.e. 0–12-month lag) extrinsic variable is used.

Such effects may be alleviated through a number of recent developments in resilience studies, which, instead of using the space-for-time approach for mapping autocorrelation, have developed statistical methods to investigate the changing characteristics of autocorrelation through time. For example, Liu et al. (2019) successfully used temporal correlation changes to predict forest mortality with remote sensing data after correcting for temporal variation of other components, including intrinsic stochastic noise, long-term trends and the seasonality. This approach is an extension of the 'moving-window' approaches which have commonly been used for addressing reduced resilience over time (e.g. Dakos et al., 2008), and which have been applied under a range of settings to propose decreases in resilience in Earth system time series, such as lake eutrophication (Ortiz et al., 2020) and palaeoclimate time series (Dakos et al., 2008). As remote sensing time series become longer, it may become more and more feasible to assess these changing time series components at a global scale. In comparison to a space-for-time approach, such dynamic approaches may better reflect the changing sensitivity of various ecosystem components as the underlying state variables shift, in particular to against a backdrop of changing anthropogenic and other climate forcing variables.

Finally, we propose that future vegetation memory research may be greatly enhanced by adopting resilience concepts which have recently been developed for other ecological applications such as the concepts within the demographic resilience proposed by Capdevila et al. (2020). This resilience framework explicitly quantifies resistance and recovery of a population or ecosystem in response to a discrete perturbation event. Assessing response of a system to a discrete perturbation event than cumulative environmental conditions like we have done may prove successful in distinguishing intrinsic from extrinsic vegetation memory components in the future.

5 | CONCLUSIONS

Our vegetation memory revealed patterns of intrinsic and extrinsic vegetation memory strength and length across global dryland regions. However, in spite of incorporation of novel climate reanalysis data to reveal patterns of vegetation memory at a global scale, we

found major differences in the relative strength of intrinsic vegetation memory compared to previous studies. Thus, our study reveals the sensitivity of this variable to the incorporation of other extrinsic forcing variables, and the current understanding of intrinsic vegetation memory as a proxy of engineering resilience/recovery speed may be an oversimplification. A critical next step will be to develop a more refined selection of variables and localised identification of vegetation memory processes.

CONFLICT OF INTEREST

The authors declare no conflict of interest associated with this work.

AUTHORS' CONTRIBUTIONS

E.K and A.W.R.S. developed the framework used in this study; E.K. created all R scripts necessary for analyses with input by A.W.R.S.; R.D. created scripts for downloading ERA5 data and introduced statistical downscaling to the methodology; E.K. led analysis with contributions from A.W.R.S. and R.D. All authors contributed critically to the drafts and gave the final approval for publication.

PEER REVIEW

The peer review history for this article is available at https://publons.com/publon/10.1111/1365-2745.13891.

DATA AVAILABILITY STATEMENT

All data sources are freely available, and the analysis is fully reproducible using the scripts provided at https://github.com/ErikKusch/Vegetation-Memory. The results shown in the main text can be reproduced following the code in Zenodo: https://doi.org/10.5281/zenodo.5031523 (Kusch, 2021) and using the data provided at Dryad: https://doi.org/10.5061/dryad.k98sf7m6d (Kusch et al., 2021).

ORCID

Erik Kusch https://orcid.org/0000-0002-4984-7646
Richard Davy https://orcid.org/0000-0001-9639-5980
Alistair W. R. Seddon https://orcid.org/0000-0002-8266-0947

REFERENCES

Abel, C., Horion, S., Tagesson, T., De Keersmaecker, W., Seddon, A. W. R., Abdi, A. M., & Fensholt, R. (2021). The human–environment nexus and vegetation–rainfall sensitivity in tropical drylands. *Nature Sustainability*, 4(1), 25–32. https://doi.org/10.1038/s41893-020-00597-z

Adeel, Z., Safriel, U., Niemeijer, D., White, R., de Kalbermatten, G., Glantz, M., Salem, B., Scholes, B., Niamir-Fuller, M., Ehui, S., & Yapi-Gnaore, V. (2005). Ecosystems and human well-being—Desertification synthesis. Retrieved from https://www.millenniumassessment.org/documents/document.355.aspx.pdf

Adier, P. B., Salguero-Gómez, R., Compagnoni, A., Hsu, J. S., Ray-Mukherjee, J., Mbeau-Ache, C., & Franco, M. (2014). Functional traits explain variation in plant lifehistory strategies. *Proceedings of the National Academy of Sciences of the United States of America*, 111(2), 740–745. https://doi.org/10.1073/pnas.1315179111

Allen, C. D., Macalady, A. K., Chenchouni, H., Bachelet, D., McDowell, N., Vennetier, M., Kitzberger, T., Rigling, A., Breshears, D. D., Hogg, E. H., Gonzalez, P., Fensham, R., Zhang, Z., Castro, J., Demidova, N., Lim, J.-H., Allard, G., Running, S. W., Semerci, A., & Cobb, N. S.

(2010). A global overview of drought and heat-induced tree mortality reveals emerging climate change risks for forests. *Forest Ecology and Management*, 259(4), 660–684. https://doi.org/10.1016/j.foreco.2009.09.001

Archibald, S., Hempson, G. P., & Lehmann, C. (2019). A unified framework for plant life-history strategies shaped by fire and herbivory. *New Phytologist*, 224(4), 1490–1503. https://doi.org/10.1111/nph.15986

Balsamo, G., Albergel, C., Beljaars, A., Boussetta, S., Brun, E., Cloke, H., Dee, D., Dutra, E., Muñoz-Sabater, J., Pappenberger, F., de Rosnay, P., Stockdale, T., & Vitart, F. (2015). ERA-interim/land: A global land surface reanalysis data set. *Hydrology and Earth System Sciences*, 19(1), 389–407. https://doi.org/10.5194/hess-19-389-2015

Broich, M., Tulbure, M. G., Verbesselt, J., Xin, Q., & Wearne, J. (2018). Quantifying Australia's dryland vegetation response to flooding and drought at sub-continental scale. *Remote Sensing of Environment*, 212(April), 60–78. https://doi.org/10.1016/j.rse.2018.04.032

Calvet, J.-C., & Barbu, A. (2015). *Gio Global Land Component—Lot I 'Operation of the Global Land Component': Cross-Cutting Quality Monitoring Report*.

Capdevila, P., Stott, I., Beger, M., & Salguero-Gómez, R. (2020). Towards a comparative framework of demographic resilience. *Trends in Ecology & Evolution*, 35(9), 776–786. https://doi.org/10.1016/j.tree.2020.05.001

Convention on Biological Diversity. (2020). *Aichi biodiversity targets*.

Côté, I. M., & Darling, E. S. (2010). Rethinking ecosystem resilience in the face of climate change. *PLoS Biology*, 8(7), e1000438. https://doi.org/10.1371/journal.pbio.1000438

Cumming, G. S., Allen, C. R., Ban, N. C., Biggs, D., Biggs, H. C., Cumming, D. H. M., De Vos, A., Epstein, G., Etienne, M., Maciejewski, K., Mathevet, R., Moore, C., Nenadovic, M., & Schoon, M. (2015). Understanding protected area resilience: A multi-scale, social-ecological approach. *Ecological Applications*, 25(2), 299–319. https://doi.org/10.1890/13-2113.1

Dakos, V., Scheffer, M., van Nes, E. H., Brovkin, V., Petoukhov, V., & Held, H. (2008). Slowing down as an early warning signal for abrupt climate change. *Proceedings of the National Academy of Sciences of the United States of America*, 105(38), 14308–14312. https://doi.org/10.1073/pnas.0802430105

De Keersmaecker, W., Lhermitte, S., Hill, M., Tits, L., Coppin, P., & Somers, B. (2017). Assessment of regional vegetation response to climate anomalies: A case study for Australia using GIMMS NDVI time series between 1982 and 2006. *Remote Sensing*, 9(1), 34. https://doi.org/10.3390/rs9010034

De Keersmaecker, W., Lhermitte, S., Tits, L., Honnay, O., Somers, B., & Coppin, P. (2015). A model quantifying global vegetation resistance and resilience to short-term climate anomalies and their relationship with vegetation cover. *Global Ecology and Biogeography*, 24(5), 539–548. https://doi.org/10.1111/geb.12279

ECMWF. (2018a). Era5: Fifth generation of ECMWF atmospheric reanalyses of the global climate 4. Retrieved from https://cds.climate.copernicus.eu/cdsapp

ECMWF. (2018b). Part II: Data assmiliation. In *IFS documentation CY45R1*: *Vol. March* (pp. 1–103). Retrieved from https://www.ecmwf.int/node/18712

ECMWF. (2018c). Part III: Dynamics And Numerical Procedures. In *IFS Documentation CY45R1*: *Vol. March* (pp. 1–31).

ECMWF. (2018d). Part IV: Physical Processes. In *IFS Documentation CY45R1* (pp. 1–189).

Esper, J., Schneider, L., Smerdon, J. E., Schöne, B. R., & Büntgen, U. (2015). Signals and memory in tree-ring width and density data. *Dendrochronologia*, 35, 62–70. https://doi.org/10.1016/j.dendro.2015.07.001

Gamon, J. A., Field, C. B., Goulden, M. L., Griffin, K. L., Hartley, A. E., Joel, G., Penuelas, J., & Valentini, R. (1995). Relationships between

NDVI, canopy structure, and photosynthesis in three Californian vegetation types. *Ecological Applications*, 5(1), 28–41. https://doi.org/10.2307/1942049

Gazol, A., Camarero, J. J., Vicente-Serrano, S. M., Sánchez-Salguero, R., Gutiérrez, E., de Luis, M., Sangüesa-Barreda, G., Novak, K., Rozas, V., Tíscar, P. A., Linares, J. C., Martín-Hernández, N., Martínez del Castillo, E., Ribas, M., García-González, I., Silla, F., Camisón, A., Génova, M., Olano, J. M., … Galván, J. D. (2018). Forest resilience to drought varies across biomes. *Global Change Biology*, 24(5), 2143–2158. https://doi.org/10.1111/gcb.14082

Genkai-Kato, M. (2007). Regime shifts: Catastrophic responses of ecosystems to human impacts. *Ecological Research*, 22(2), 214–219. https://doi.org/10.1007/s11284-006-0304-5

Grafton, R. Q., Doyen, L., Béné, C., Borgomeo, E., Brooks, K., Chu, L., Cumming, G. S., Dixon, J., Dovers, S., Garrick, D., Helfgott, A., Jiang, Q., Katic, P., Kompas, T., Little, L. R., Matthews, N., Ringler, C., Squires, D., Steinshamn, S. I., … Wyrwoll, P. R. (2019). Realizing resilience for decision-making. *Nature Sustainability*, 2(10), 907–913. https://doi.org/10.1038/s41893-019-0376-1

Harris, A., Carr, A. S., & Dash, J. (2014). Remote sensing of vegetation cover dynamics and resilience across southern Africa. *International Journal of Applied Earth Observation and Geoinformation*, 28(1), 131–139. https://doi.org/10.1016/j.jag.2013.11.014

Hodgson, D., McDonald, J. L., & Hosken, D. J. (2015). What do you mean, 'resilient'? *Trends in Ecology & Evolution*, 30(9), 503–506. https://doi.org/10.1016/j.tree.2015.06.010

Holling, C. S. (1973). Resilience and stability of ecological systems. *Annual Review of Ecology and Systematics*, 4(1), 1–23. https://doi.org/10.1146/annurev.es.04.110173.000245

Huete, A., Didan, K., Miura, T., Rodriguez, E., Gao, X., & Ferreira, L. (2002). Overview of the radiometric and biophysical performance of the MODIS vegetation indices. *Remote Sensing of Environment*, 83(1–2), 195–213. https://doi.org/10.1016/S0034-4257(02)00096-2

Kannenberg, S. A., Schwalm, C. R., & Anderegg, W. R. L. (2020). Ghosts of the past: How drought legacy effects shape forest functioning and carbon cycling. *Ecology Letters*, 23(5), 891–901. https://doi.org/10.1111/ele.13485

Kusch, E. (2021). Data from: ErikKusch/Vegetation-Memory: Upload to Zenodo (1.0). *Zenodo*, https://doi.org/10.5281/zenodo.5031523

Kusch, E., & Davy, R. (2022). KrigR—A tool for downloading and statistically downscaling climate reanalysis data. *Environmental Research Letters*, 17(2), 024005. https://doi.org/10.1088/1748-9326/ac48b3

Kusch, E., Davy, R., & Seddon, A. W. R. (2021). Global dryland vegetation memory—Data Repository. https://doi.org/10.5061/dryad.k98sf7m6d

Liu, L., Zhang, Y., Wu, S., Li, S., & Qin, D. (2018). Water memory effects and their impacts on global vegetation productivity and resilience. *Scientific Reports*, 8(1), 1–9. https://doi.org/10.1038/s41598-018-21339-4

Liu, Y., Kumar, M., Katul, G. G., & Porporato, A. (2019). Reduced resilience as an early warning signal of forest mortality. *Nature Climate Change*, 9(11), 880–885. https://doi.org/10.1038/s41558-019-0583-9

Lloret, F., Keeling, E. G., & Sala, A. (2011). Components of tree resilience: Effects of successive low-growth episodes in old ponderosa pine forests. *Oikos*, 120(12), 1909–1920. https://doi.org/10.1111/j.1600-0706.2011.19372.x

Macias-Fauria, M., Seddon, A. W. R., Benz, D., Long, P. R., & Willis, K. (2014). Spatiotemporal patterns of warming. *Nature Climate Change*, 4(10), 845–846. https://doi.org/10.1038/nclimate2372

Martens, B., Schumacher, D. L., Wouters, H., Muñoz-Sabater, J., Verhoest, N. E. C., & Miralles, D. G. (2020). Evaluating the land-surface energy partitioning in ERA5. *Geoscientific Model Development*, 13(9), 4159–4181. https://doi.org/10.5194/gmd-13-4159-2020

McGill, R., Tukey, J. W., & Larsen, W. A. (1978). Variations of box plots. *The American Statistician*, 32(1), 12. https://doi.org/10.2307/2683468

Millennium Ecosystem Assessment. (2005a). Dryland systems. In *Ecosystems and human well-being: Current state and trends* (pp. 625–662). Island Press.

Millennium Ecosystem Assessment. (2005b). Millennium ecosystem assessment: MA ecosystems. https://doi.org/10.7927/H4KW5CZ6

Neubert, M. G., & Caswell, H. (1997). Alternatives to resilience for measuring the responses of ecological systems to perturbations. *Ecology*, 78(3), 653–665. https://doi.org/10.1890/0012-9658(1997)078[0653:ATRFMT]2.0.CO;2

Nielsen, R. L., James, J. J., & Drenovsky, R. E. (2019). Functional traits explain variation in chaparral shrub sensitivity to altered water and nutrient availability. *Frontiers in Plant Science*, 10(April), 1–15. https://doi.org/10.3389/fpls.2019.00505

Nyström, M., & Folke, C. (2001). Spatial resilience of coral reefs. *Ecosystems*, 4(5), 406–417. https://doi.org/10.1007/s10021-001-0019-y

Ogle, K., Barber, J. J., Barron-Gafford, G. A., Bentley, L. P., Young, J. M., Huxman, T. E., Loik, M. E., & Tissue, D. T. (2015). Quantifying ecological memory in plant and ecosystem processes. *Ecology Letters*, 18(3), 221–235. https://doi.org/10.1111/ele.12399

Ortiz, D., Palmer, J., & Wilkinson, G. (2020). Detecting changes in statistical indicators of resilience prior to algal blooms in shallow eutrophic lakes. *Ecosphere*, 11(10), 1–14. https://doi.org/10.1002/ecs2.3200

Papagiannopoulou, C., Di Miralles, G., Decubber, S., Demuzere, M., Verhoest, N. E. C., Dorigo, W. A., & Waegeman, W. (2017). A non-linear granger-causality framework to investigate climate–vegetation dynamics. *Geoscientific Model Development*, 10(5), 1945–1960. https://doi.org/10.5194/gmd-10-1945-2017

Pettorelli, N., Vik, J. O., Mysterud, A., Gaillard, J.-M., Tucker, C. J., & Stenseth, N. C. (2005). Using the satellite-derived NDVI to assess ecological responses to environmental change. *Trends in Ecology & Evolution*, 20(9), 503–510. https://doi.org/10.1016/j.tree.2005.05.011

Pimm, S. L., Donohue, I., Montoya, J. M., & Loreau, M. (2019). Measuring resilience is essential to understand it. *Nature Sustainability*, 2(10), 895–897. https://doi.org/10.1038/s41893-019-0399-7

Prince, S. D., & Goward, S. N. (1995). Global primary production: A remote sensing approach. *Journal of Biogeography*, 22(4/5), 815. https://doi.org/10.2307/2845983

Sabater, J. M. (2021). ERA5-land: A new state-of- the-art global land surface reanalysis dataset. *Earth System Science Data*, 13, 4349–4383. https://doi.org/10.5194/essd-13-4349-2021

Scheffer, M., Bascompte, J., Brock, W. A., Brovkin, V., Carpenter, S. R., Dakos, V., Held, H., Van Nes, E. H., Rietkerk, M., & Sugihara, G. (2009). Early-warning signals for critical transitions. *Nature*, 461(7260), 53–59. https://doi.org/10.1038/nature08227

Scheffer, M., & Carpenter, S. R. (2003). Catastrophic regime shifts in ecosystems: Linking theory to observation. *Trends in Ecology & Evolution*, 18(12), 648–656. https://doi.org/10.1016/j.tree.2003.09.002

Scheffer, M., Carpenter, S. R., Dakos, V., & van Nes, E. H. (2015). Generic indicators of ecological resilience: Inferring the chance of a critical transition. *Annual Review of Ecology, Evolution, and Systematics*, 46(1), 145–167. https://doi.org/10.1146/annurev-ecolsys-112414-054242

Seddon, A. W. R., Macias-Fauria, M., Long, P. R., Benz, D., & Willis, K. J. (2016). Sensitivity of global terrestrial ecosystems to climate variability. *Nature*, 531(7593), 229–232. https://doi.org/10.1038/nature16986

Senf, C., & Seidl, R. (2018). Natural disturbances are spatially diverse but temporally synchronized across temperate forest landscapes in Europe. *Global Change Biology*, 24(3), 1201–1211. https://doi.org/10.1111/gcb.13897

Smith, A. P., Bond-Lamberty, B., Benscoter, B. W., Tfaily, M. M., Hinkle, C. R., Liu, C., & Bailey, V. L. (2017). Shifts in pore connectivity from precipitation versus groundwater rewetting increases soil carbon

loss after drought. *Nature Communications*, 8(1), 1335. https://doi.org/10.1038/s41467-017-01320-x

Spears, B. M., Futter, M. N., Jeppesen, E., Huser, B. J., Ives, S., Davidson, T. A., Adrian, R., Angeler, D. G., Burthe, S. J., Carvalho, L., Daunt, F., Gsell, A. S., Hessen, D. O., Janssen, A. B. G., Mackay, E. B., May, L., Moorhouse, H., Olsen, S., Søndergaard, M., ... Thackeray, S. J. (2017). Ecological resilience in lakes and the conjunction fallacy. *Nature Ecology & Evolution*, 1(11), 1616–1624. https://doi.org/10.1038/s41559-017-0333-1

Standish, R. J., Hobbs, R. J., Mayfield, M. M., Bestelmeyer, B. T., Suding, K. N., Battaglia, L. L., Eviner, V., Hawkes, C. V., Temperton, V. M., Cramer, V. A., Harris, J. A., Funk, J. L., & Thomas, P. A. (2014). Resilience in ecology: Abstraction, distraction, or where the action is? *Biological Conservation*, 177, 43–51. https://doi.org/10.1016/j.biocon.2014.06.008

Stow, D. A., Hope, A., McGuire, D., Verbyla, D., Gamon, J., Huemmrich, F., Houston, S., Racine, C., Sturm, M., Tape, K., Hinzman, L., Yoshikawa, K., Tweedie, C., Noyle, B., Silapaswan, C., Douglas, D., Griffith, B., Jia, G., Epstein, H., ... Myneni, R. (2004). Remote sensing of vegetation and land-cover change in Arctic tundra ecosystems. *Remote Sensing of Environment*, 89(3), 281–308. https://doi.org/10.1016/j.rse.2003.10.018

Sustainable Development Goals. (2020). Retrieved from United Nations website: https://www.un.org/sustainabledevelopment/sustainable-development-goals/

Tang, W., Qin, J., Yang, K., Zhu, F., & Zhou, X. (2021). Does ERA5 outperform satellite products in estimating atmospheric downward longwave radiation at the surface? *Atmospheric Research*, 252(April), 105453. https://doi.org/10.1016/j.atmosres.2021.105453

Tarek, M., Brissette, F. P., & Arsenault, R. (2020). Evaluation of the ERA5 reanalysis as a potential reference dataset for hydrological modelling over North America. *Hydrology and Earth System Sciences*, 24(5), 2527–2544. https://doi.org/10.5194/hess-24-2527-2020

Tian, F., Brandt, M., Liu, Y. Y., Rasmussen, K., & Fensholt, R. (2017). Mapping gains and losses in woody vegetation across global tropical drylands. *Global Change Biology*, 23(4), 1748–1760. https://doi.org/10.1111/gcb.13464

Verbesselt, J., Umlauf, N., Hirota, M., Holmgren, M., Van Nes, E. H., Herold, M., Zeileis, A., & Scheffer, M. (2016). Remotely sensed resilience of tropical forests. *Nature Climate Change*, 6(11), 1028–1031. https://doi.org/10.1038/nclimate3108

Vicente-Serrano, S. M., Gouveia, C., Camarero, J. J., Beguería, S., Trigo, R., Lopez-Moreno, J. I., Azorin-Molina, C., Pasho, E., Lorenzo-Lacruz, J., Revuelto, J., Moran-Tejeda, E., & Sanchez-Lorenzo, A. (2013). Response of vegetation to drought time-scales across global land biomes. *Proceedings of the National Academy of Sciences of the United States of America*, 110(1), 52–57. https://doi.org/10.1073/pnas.1207068110

Wan, L., Tong, J., Zhou, J., Guo, H., Cui, M., Liu, Y., Ning, L., & Tang, F. (2016). Variation of vegetation ecological water consumption and its response to vegetation coverage changes in the rocky desertification areas in South China. *PLoS ONE*, 11(10), e0163566. https://doi.org/10.1371/journal.pone.0163566

Wang, D., Heckathorn, S. A., Mainali, K., & Tripathee, R. (2016). Timing effects of heat-stress on plant ecophysiological characteristics and growth. *Frontiers in Plant Science*, 7(November), 1–11. https://doi.org/10.3389/fpls.2016.01629

Wen, Y., Liu, X., Yang, J., Lin, K., & Du, G. (2019). NDVI indicated interseasonal non-uniform time-lag responses of terrestrial vegetation growth to daily maximum and minimum temperature. *Global and Planetary Change*, 177, 27–38. https://doi.org/10.1016/j.gloplacha.2019.03.010

Wickham, H. (2016). ggplot2: Elegant graphics for data analysis. Retrieved from https://ggplot2.tidyverse.org

World Wildlife Fund. (2020). Terrestrial ecoregions of the world. Retrieved from http://omap.africanmarineatlas.org/BIOSPHERE/data/note_areas_sp/Ecoregions_Ecosystems/WWF_Ecoregions/WWFecoregions.htm

Xu, C., Van Nes, E. H., Holmgren, M., Kéfi, S., & Scheffer, M. (2015). Local facilitation may cause tipping points on a landscape level preceded by early-warning indicators. *The American Naturalist*, 186(4), E81–E90. https://doi.org/10.1086/682674

Yin, D., Li, X., Huang, Y., Si, Y., & Bai, R. (2015). Identifying vegetation dynamics and sensitivities in response to water resources Management in the Heihe River Basin in China. *Advances in Meteorology*, 2015, 1–12. https://doi.org/10.1155/2015/861928

SUPPORTING INFORMATION

Additional supporting information may be found in the online version of the article at the publisher's website.